

Sensitivity analysis of biophysically-detailed tripartite synapse model

Ippa Seppälä* Tiina Manninen* Marja-Leena Linne*

* *Computational Neuroscience Group, Faculty of Medicine and Health Technology, Tampere University, Tampere, Finland (e-mail: tiina.manninen@tuni.fi, marja-leena.linne@tuni.fi)*

Abstract: Now that mathematical models are becoming larger and biophysically more detailed, understanding how each variable, parameter, and equation affects the outcome of the model becomes paramount. In this study, we performed sensitivity analysis of a biophysically-detailed tripartite synapse model that includes three cells, the pre- and postsynaptic neurons and the astrocyte, using the Uncertainpy python toolbox. Because of the computational burden, we were able to run the sensitivity analysis on sets of three to four parameters at a time. The analysis revealed eight sensitive parameters, which we then analyzed in more detail. In the end, we found two parameters to be the most sensitive; one of which arose from the postsynaptic neuron and the other from the astrocyte. Further analysis with larger parameter cohorts would be needed to make any conclusions on the robustness of the model, but all in all our findings were promising.

Copyright © 2022 The Authors. This is an open access article under the CC BY-NC-ND license (<https://creativecommons.org/licenses/by-nc-nd/4.0/>)

Keywords: Computational model, sensitivity analysis, simulation, synapse, Uncertainpy

1. INTRODUCTION

Models in computational neuroscience are growing ever larger. The emergence of new information about intricate pathways and molecular functions is accompanied by large amounts of new data from experiments and simulations, and these data are used to construct even more detailed models of the brain. To capture as much details as possible, large biophysically realistic models are needed, but they run into problems when the number of parameters and variables increases. The overparameterization often results in uncertainty in the parameters themselves as well as the predictions computed using the model (Eriksson et al., 2019). Thus, it is becoming more and more pertinent to perform sensitivity and uncertainty analysis on such models. This allows us to perform better informed predictions by finding the most essential parameters and understanding their relationship to the outcome.

By sensitivity analysis we mean the quantification of the uncertainty in the model output that a particular uncertain parameter is responsible for. Sensitivity analysis methods can be divided into local and global methods (see, e.g., Zi, 2011; Borgonovo and Plischke, 2016). With local methods, the analysis is done in close vicinity of a certain chosen point in parameter space, whereas with global methods, the analysis is done by assigning probability distributions for the parameter space.

Several sensitivity analysis tools exist (see, e.g., Tennøe et al., 2018; Santos et al., 2021). In this study, we used Uncertainpy toolbox (Tennøe et al., 2018) which provides two different global methods for its sensitivity analysis, the quasi-Monte Carlo method and the polynomial chaos expansion. In the standard Monte Carlo method, a set of parameters is pseudo-randomly selected from the joint multivariate probability density function of all the uncer-

tain parameters under review. The model is evaluated for each pseudo-random set of parameters, which means that it will be evaluated thousands of times and the statistical metrics (mean and variance) will be calculated for the output after each evaluation. The quasi-Monte Carlo method uses variance reduction methods to allow the parameters to be sampled more evenly and thus giving better coverage of the statistics with less samples. As long as the number of uncertain parameters is sufficiently small, the quasi-Monte Carlo method outperforms the standard Monte Carlo version. Still, if the number of parameters is kept relatively low (e.g., lower than 20), the polynomial chaos expansion will be far faster than even the quasi-Monte Carlo (Tennøe et al., 2018) as it belongs to the class of efficient polynomial approximation methods. Due to the speed limitations, it is advised that with larger models such as those common in computational neuroscience, sensitivity analysis should be performed on smaller subsets of parameters at a time. This will of course limit the amount of information of the sensitivity in the context of the entire system, as the number of parameters whose value is simultaneously variable is restricted. In the polynomial chaos expansion, the model is approximated by a polynomial expansion. Uncertainpy first looks for the orthogonal polynomials and then estimates the expansion coefficients. There are two classes of nonintrusive methods for doing this, both of which are implemented in Uncertainpy.

With the Uncertainpy toolbox, we performed sensitivity analysis of a biophysically-detailed tripartite synapse model (Manninen et al., 2020). Quantifying the sensitivity (and uncertainty) of the model parameters allowed us to assess the robustness of the model as well as its well-suitedness to predict spike-timing-dependent long-term depression (t-LTD). We were able to run the sensitivity analysis on sets of three to four parameters at a time.

2. METHODS

One can think of a computational model as a system M that relies on space x , time t , uncertain parameters $Q = [q_1, q_2, \dots, q_m]$ and results in an output Y such that

$$Y = M(x, t, Q). \quad (1)$$

Each uncertain parameter has a probability distribution P_q that the parameter will be drawn from. The uncertainty of a parameter can be caused by experimental measurements, uncertain theoretical values, or other variations. These variations give rise to a probability distribution for each uncertain parameter.

The Uncertainty toolbox can use two different methods for its sensitivity analysis, the quasi-Monte Carlo method and the polynomial chaos expansion. The Uncertainty toolbox relies upon the commonly used Sobol sensitivity indices method (Sobol, 2001) calculating both first-order and total-order Sobol indices.

2.1 Quasi-Monte Carlo methods

The statistical metrics (mean and variance) will be calculated for the output after each evaluation. The quasi-Monte Carlo method uses a low-discrepancy sequence to select the samples of uncertain parameters with which the model will be evaluated. Compared to the pseudo-random selection used by the standard Monte Carlo method, this allows for the samples to be picked out more evenly, giving better coverage of the statistics of the probability distribution using less samples (Tennøe et al., 2018). The quasi-Monte Carlo method outperforms the standard Monte Carlo approach if the number of uncertain parameters is sufficiently small.

2.2 Polynomial chaos expansion

Using the polynomial chaos expansion method, the model is approximated by a polynomial expansion in which the polynomials are orthogonal to the probability density function. This approximation is given by

$$M \approx \hat{M}(x, t, Q) = \sum_{n=0}^{N_p-1} c_n(x, t) \phi_n(Q), \quad (2)$$

where M is again the model system, x the set of variables, and Q the set of uncertain parameters. Uncertainty first looks for the orthogonal polynomials ϕ_n and then estimates the expansion coefficients c_n . The number of expansion factors N_p is given by

$$N_p = \binom{d+p}{p}, \quad (3)$$

where p represents the polynomial order and d the number of uncertain parameters. There are two classes of nonintrusive methods for doing this, both of which are implemented in Uncertainty: point collocation method, which is the default method, and the pseudo-spectral projection methods.

The point collocation method is based on demanding the polynomial approximation to be equal to the model output at a set of collocation nodes drawn from the probability density function. To put it simply, a set of samples are

chosen and at those points the approximation is forced to be equal to the original model output. This results in a set of linear equations for the polynomial coefficient c_n . These equations can then be solved using regression methods, the one used by Uncertainty being the Tikhonov regularization (Tikhonov, 1943).

Pseudo-spectral projection methods are based on least squares minimization in orthogonal polynomial space. This method finds the expansion coefficients c_n by numerical integration using a quadrature scheme. Uncertainty uses Leja quadrature to find appropriate weights and the nodes at which the model will be evaluated. Smolyak sparse grids are used to reduce the number of these nodes to speed up the calculation. The pseudo-spectral projection method is used only when requested by the user and not by default.

2.3 Tripartite synapse model

We performed sensitivity analysis of the tripartite synapse model by Manninen et al. (2020) which was constructed for t-LTD in the developing somatosensory cortex. The model includes major biophysical and biochemical mechanisms for the three cells, the one-compartmental presynaptic spiny stellate cell, two-compartmental postsynaptic pyramidal cell, and one-compartmental fine astrocyte process. The model has altogether about 80 differential equations and 170 parameters.

2.4 Chosen uncertain parameters

Out of the about 170 model parameters, 26 parameters of interest were studied with the sensitivity analysis. These parameters were specifically chosen for one of two reasons; either their sensitivity was made evident during the construction of the original model or there was no biologically relevant value available for them in the literature at the time. During the sensitivity analysis, we used a uniform distribution for all uncertain parameters with the minimum value being 90 % and the maximum value 110 % of the original values given in Tables 1–3.

2.5 Model stimulus

Due to the complexity of the studied model, adjustments to the simulations needed to be made. The model, as described in Section 2.3, was originally simulated with a post-pre pairing protocol for 500 s with a 5 s gap between each pairing stimulus of the post- and presynaptic neurons (Min and Nevian, 2012; Banerjee et al., 2014). Furthermore, before the pairing protocol was started there was originally a 20 s period where no stimulus was given to either of the neurons. In the pairing protocol, the stimuli were given to the pre- and postsynaptic neurons with a small temporal difference in between. This temporal difference ranged from -10 to -200 ms, as the postsynaptic stimulus was given first before the presynaptic stimulus (Banerjee et al., 2014), in 10 ms increments; so, 20 different temporal differences in total.

Here we simulated the model for five post-pre pairings without the 20 s idle period before the initial stimulus, thus the simulation time was 25 s. Most of the analyses were performed using a temporal difference of -10 ms between

Table 1. Analyzed parameters of the presynaptic neuron

Parameter	Explanation	Value	Unit
X_total_pre	Total concentration of presynaptic protein affecting vesicular release	0.1	μM
p1_pre	Rate constant for presynaptic protein activation affecting vesicular release	0.00003	$\frac{1}{\text{ms}}$
N_pre	Number of readily releasable presynaptic vesicles	2	
kd2_f_pre	Rate constant into desensitized state of presynaptic N-methyl-D-aspartate receptors (NMDARs)	0.0112	$\frac{1}{\text{ms}}$
kd1_f_pre	Rate constant into desensitized state of presynaptic NMDARs	0.055	$\frac{1}{\text{ms}}$
gNMDAR_pre	Maximum conductance of presynaptic NMDARs per unit area	0.1	$\frac{\text{mS}}{\text{cm}^2}$
K_rel_pre	Presynaptic calcium (Ca^{2+}) concentration producing half occupation used in calculation of glutamate release	5	μM
KA_pre	Presynaptic calcineurin concentration producing half occupation	2	μM
k_f_pre	Presynaptic facilitation rate constant	0.0075	$\frac{1}{\text{ms}}$
k2_pre	Rate constant for inactivation of presynaptic calcineurin	0.002	$\frac{1}{\text{ms}}$
k1_pre	Rate constant for Ca^{2+} activation of presynaptic calcineurin	0.001	$\frac{1}{\mu\text{M}^3 \text{ms}}$
C_thr_pre	Ca^{2+} threshold concentration of glutamate release in presynaptic neuron	3	μM
f_glu_pre	Factor representing spillover of glutamate from synaptic cleft to extrasynaptic space	0.1	

Table 2. Analyzed parameters of the postsynaptic neuron

Parameter	Explanation	Value	Unit
v_SERCA_post	Maximum rate of Ca^{2+} uptake by postsynaptic sarco/endoplasmic reticulum Ca^{2+} -ATPase (SERCA)	0.003	$\frac{\mu\text{M}}{\text{ms}}$
k_Glu_f_post	Reaction rate for glutamate uptake by postsynaptic metabotropic glutamate receptors	0.2	$\frac{1}{\text{ms}}$
k_Ca_PLC1_f_post	Metabotropic glutamate receptor and endocannabinoid 2-arachidonoylglycerol (2-AG) related parameter	0.002	$\frac{1}{\mu\text{M} \text{ms}}$
gCaLHVA_dend_post	Maximum conductance of postsynaptic L-type high-voltage-activated Ca^{2+} current in the dendrite per unit area	0.23	$\frac{\text{mS}}{\text{cm}^2}$
gCaLLVA_dend_post	Maximum conductance of postsynaptic L-type low-voltage-activated Ca^{2+} current in the dendrite per unit area	0.23	$\frac{\text{mS}}{\text{cm}^2}$
gNMDAR_post	Maximum conductance of postsynaptic NMDARs per unit area	0.001	$\frac{\text{mS}}{\text{cm}^2}$
B_post	Postsynaptic fast buffering factor	0.5	
v_IP3R_post	Maximum rate of Ca^{2+} release via postsynaptic inositol 1,4,5-trisphosphate (IP_3) receptors	0.01	$\frac{1}{\text{ms}}$
v_PMCA_post	Maximum rate of Ca^{2+} uptake by postsynaptic plasma membrane Ca^{2+} -ATPase (PMCA) per unit area	8×10^{-11}	$\frac{\mu\text{Mol}}{\text{ms cm}^2}$

Table 3. Analyzed parameters of the astrocyte

Parameter	Explanation	Value	Unit
C_thr_astro	Ca^{2+} threshold concentration of glutamate exocytosis in astrocytes	0.3	μM
N_astro	Number of readily releasable astrocytic vesicles	4	
r_IP3_astro	Rate constant of astrocytic IP_3 production	0.0008	$\frac{1}{\text{ms}}$
v_SERCA_astro	Maximum rate of Ca^{2+} uptake by astrocytic SERCA pump	0.0007	$\frac{\mu\text{M}}{\text{ms}}$

the post-pre pairing, but we were able to run the analysis with values up to -200 ms.

3. RESULTS

Due to limitations in the computing resources, we chose the most important parameters from each of the three cell types in the model (Tables 1–3) and compared them against three state variables as outputs; the concentration of glutamate in the synaptic cleft ($[\text{Glu}]_{\text{synleft}}$), the concentration of postsynaptic endocannabinoid 2-arachidonoylglycerol ($[\text{2-AG}]_{\text{post}}$), and the concentration of glutamate in the extrasynaptic space ($[\text{Glu}]_{\text{extsyn}}$).

We analyzed the sensitivity of the uncertain parameters with the polynomial chaos expansion method as it per-

forms much faster than the quasi-Monte Carlo method when the number of parameters is relatively low. Due to the complexity of the model, we were not able to analyze all the parameters of interest at the same time but grouped them into groups of three or four. The memory required for running the model whilst simultaneously varying more than four parameters exceeded the memory limit of the computing cluster. This only shows how large the model truly is even when the simulation time had already been shortened considerably. In this study, we focused on the first-order Sobol sensitivity index which indicates how much each uncertain parameter affects the variance of the model output. The averages of the indices can be seen in Figs. 1–6 where groupings of the parameters analyzed at the same time are indicated by different colors.

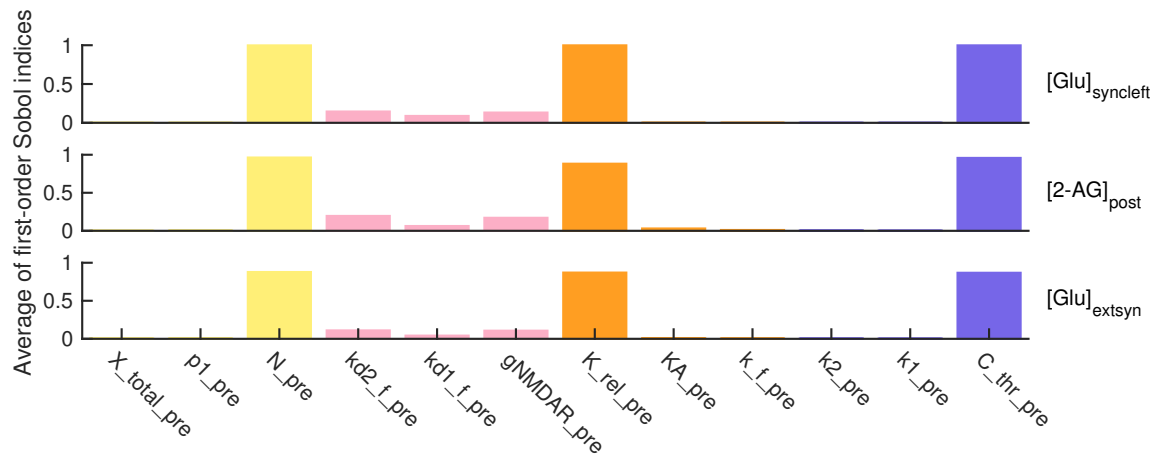


Fig. 1. The average of the first-order Sobol sensitivity indices of the presynaptic parameters. Parameters N_{pre} , K_{rel_pre} , and C_{thr_pre} were the most sensitive.

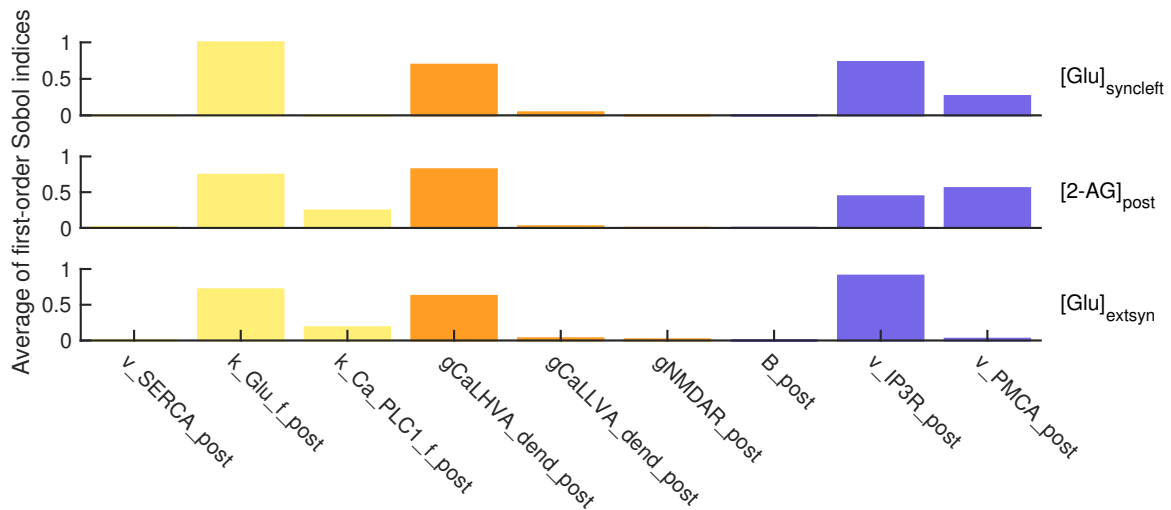


Fig. 2. The average of the first-order Sobol sensitivity indices of the postsynaptic parameters. Parameters $k_{Glu_f_post}$, $gCaLHVA_dend_post$, v_{IP3R_post} , and v_{PMCA_post} were the most sensitive.

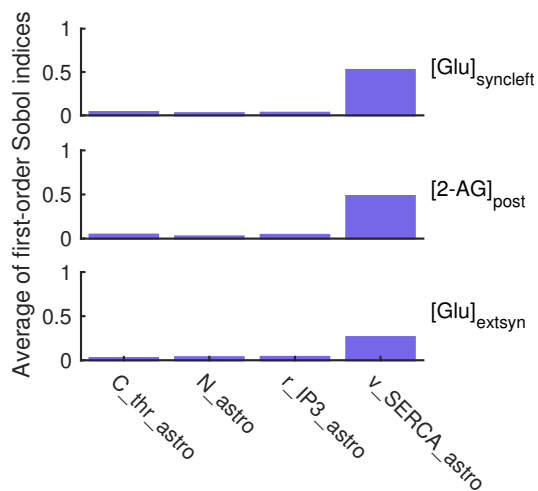


Fig. 3. The average of the first-order Sobol sensitivity indices of the astrocytic parameters. Parameter v_{SERCA_astro} was the most sensitive.

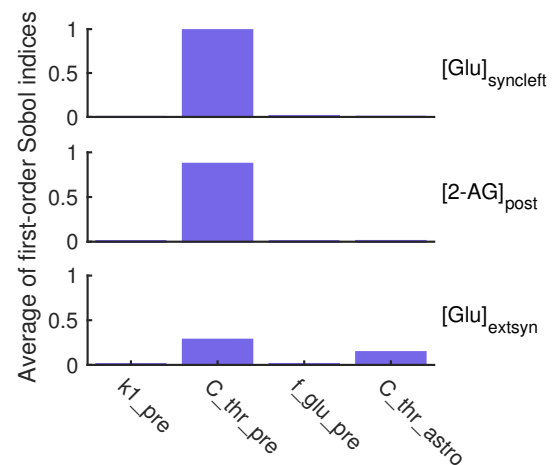


Fig. 4. The average of the first-order Sobol sensitivity indices in the case of the glutamate release parameters. Parameter C_{thr_pre} was the most sensitive.

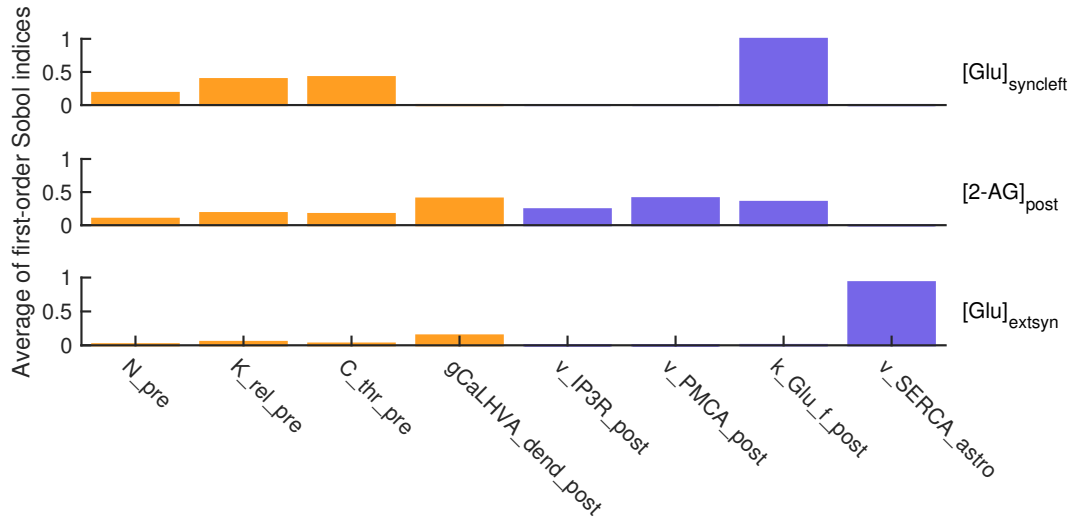


Fig. 5. The average of the first-order Sobol sensitivity indices for the most sensitive eight parameters. Parameters $k_Glu_f_post$ and v_SERCA_astro were the most sensitive.

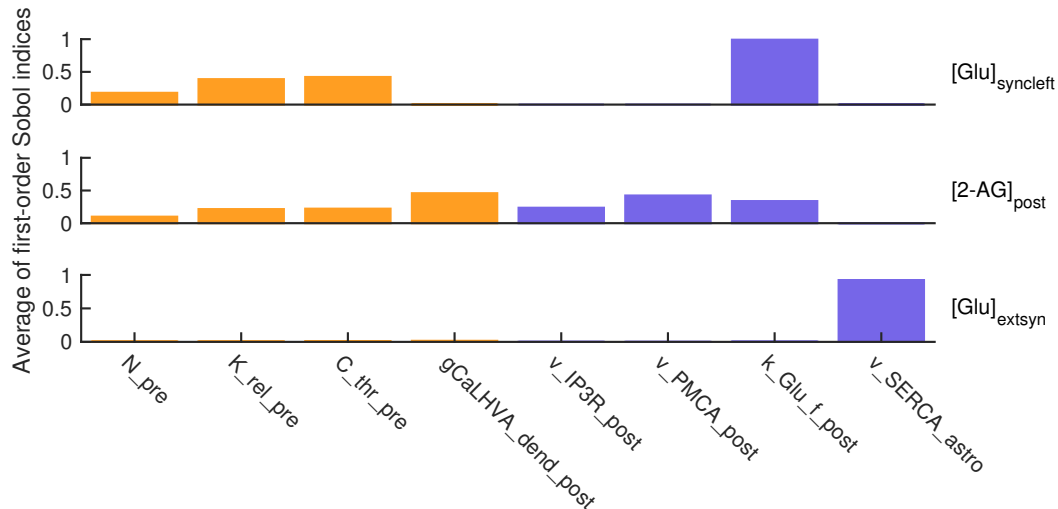


Fig. 6. The average of the first-order Sobol sensitivity indices when the time difference was -200 ms. Parameters $k_Glu_f_post$ and v_SERCA_astro were the most sensitive.

A low value of the first-order Sobol sensitivity index (close to 0) means that changes in the parameter value do not have a big effect on the model output; whereas a high value (close to 1) means that changes in the parameter value affect greatly the model output. Thus, Fig. 1 shows clearly that the parameters N_pre , K_rel_pre , and C_thr_pre were the most sensitive of the presynaptic parameters tested. Fig. 2 shows that the postsynaptic parameters $k_Glu_f_post$, $gCaLHVA_dend_post$, v_IP3R_post , and v_PMCA_post were more sensitive than the others. Fig. 3 shows that v_SERCA_astro was the most sensitive of the astrocytic parameters. To study the sensitivity of the glutamate release parameters, we next analyzed four related parameters simultaneously, namely $k1_pre$, C_thr_pre , f_glu_pre , and C_thr_astro . The parameter C_thr_pre is clearly the most sensitive parameter of these four (Fig. 4).

After having run the parameters from each cell in the small groups and for the glutamate release, altogether eight of them exceeded the value of 0.5 compared against one or

more of the three state variables (Figs. 1–4). These eight parameters were then run in two sets of four and their sensitivity indices can be found in Fig. 5. It is clear that not all the parameters that were revealed to be sensitive (exceeding the value of 0.5 for the average of first-order Sobol sensitivity indices) in their initial cohorts (Figs. 1–4) were as sensitive when grouped together with the other sensitive parameters. This indicates the importance of studying the sensitivity of parameters together rather than in smaller subsets. It would be useful to run all eight or even all the 170 parameters together, but it is not feasible with this model at this time due to computational burden.

In Figs. 1–5, the temporal difference between the post- and presynaptic stimuli was set to -10 ms, when in the original model it ranged between -10 ms and -200 ms. Because we could not know what effect this has on the sensitivity of the parameters, we decided to also test the time difference -200 ms. We did this with the eight most sensitive parameters found in the case of -10 ms. We then compared the averages of the first-order Sobol sensitivity

indices of those parameters when the simulations were run using the two temporal differences (−10 ms and −200 ms). Only slight changes in some of the parameters were visible in the Sobol sensitivity indices. For example, the sensitivity of the parameters `K_rel_pre`, `C_thr_pre`, and `gCaLHVA_dend_post` had marginally higher values in the case of −10 ms than in the case of −200 ms when compared against the concentration of glutamate in the extrasynaptic space (Figs. 5 and 6).

4. DISCUSSION AND CONCLUSIONS

The sensitivity analysis we performed with the Uncertainty toolbox revealed eight sensitive parameters. These included the parameters `N_pre`, `K_rel_pre`, and `C_thr_pre` from the presynaptic neuron, the parameters `gCaLHVA_dend_post`, `v_IP3R_post`, `v_PMCA_post`, and `k_Glu_f_post` from the postsynaptic neuron, and the parameter `v_SERCA_astro` from the astrocyte. All the studied parameters and their explanations can be found in Tables 1–3. The sensitivity indices for all the parameters tested can be found in Figs. 1–4. These parameters were mostly studied in separate simulation runs because we were only able to test three to four parameters simultaneously. After identifying the eight sensitive parameters, we analyzed them again four parameters at a time in order to see how their sensitivity was related to each other (Figs. 5 and 6). These final simulations revealed that the parameters `k_Glu_f_post` and `v_SERCA_astro` were the most sensitive of all the parameters studied here.

This was rather surprising, as during the construction of the model the parameters `k_Glu_f_post` and `v_SERCA_astro` were not considered to be among the most influential parameters of the model. One of these parameters arose from the most biophysically-detailed cell of the whole tripartite synapse model, the postsynaptic neuron, and the other from the simplest cell, the astrocyte. More in-depth analysis with larger sets of parameters run simultaneously would be needed to better assess the robustness and well-suitedness of the model for the study of t-LTD. Still these preliminary results are promising and could indicate that the model does indeed conform to the biophysical behavior of the actual cellular system.

Of the Uncertainty package itself (Tennøe et al., 2018), it can be concluded that it was fairly easy to implement even for such a large model. Due to the black box approach, Uncertainty is versatile and flexible, and can thus be utilized for various types of models. The computational burden is considerable, but this could be remedied by vetting the parameters under study with care, and by using computing platforms with enough capacity.

In summary, we conclude that we used one of the most complex neuroscience models for a synapse constructed to explain t-LTD phenomena (Manninen et al., 2020) and performed sensitivity analysis on 26 of its parameter values against the three outputs of the model. We found out that current sensitivity (uncertainty) analysis tools are not yet fully suitable for such complex models, at least to perform the full sensitivity analysis of all parameters simultaneously. Sensitivity analysis will become even more important in the future as the use of biophysically-detailed models is becoming commonplace in the study of human

health and diseases as well as the development of targeted therapies.

ACKNOWLEDGEMENTS

This research has received funding from the European Union's Horizon 2020 Framework Programme for Research and Innovation under the Specific Grant Agreement Nos. 720270 (Human Brain Project SGA1), 785907 (Human Brain Project SGA2), and 945539 (Human Brain Project SGA3), and the Academy of Finland (decision Nos. 297893, 318879, 326494, 326495, and 345280).

REFERENCES

- Banerjee, A., González-Rueda, A., Sampaio-Baptista, C., Paulsen, O., and Rodríguez-Moreno, A. (2014). Distinct mechanisms of spike timing-dependent LTD at vertical and horizontal inputs onto L2/3 pyramidal neurons in mouse barrel cortex. *Physiol. Rep.*, 2(3), e00271. doi:10.1002/phy2.271.
- Borgonovo, E. and Plischke, E. (2016). Sensitivity analysis: A review of recent advances. *Eur. J. Oper. Res.*, 248(3), 869–887. doi:10.1016/j.ejor.2015.06.032.
- Eriksson, O., Jauhiainen, A., Maad Sasane, S., Kramer, A., Nair, A.G., Sartorius, C., and Hellgren Kotaleski, J. (2019). Uncertainty quantification, propagation and characterization by Bayesian analysis combined with global sensitivity analysis applied to dynamical intracellular pathway models. *Bioinformatics*, 35(2), 284–292. doi:10.1093/bioinformatics/bty607.
- Manninen, T., Saudargiene, A., and Linne, M.L. (2020). Astrocyte-mediated spike-timing-dependent long-term depression modulates synaptic properties in the developing cortex. *PLoS Comput. Biol.*, 16(11), e1008360. doi:10.1371/journal.pcbi.1008360.
- Min, R. and Nevian, T. (2012). Astrocyte signaling controls spike timing-dependent depression at neocortical synapses. *Nat. Neurosci.*, 15(5), 746–753. doi:10.1038/nn.3075.
- Santos, J.P.G., Pajo, K., Trpevski, D., Stepaniuk, A., Eriksson, O., Nair, A.G., Keller, D., Hellgren Kotaleski, J., and Kramer, A. (2021). A modular workflow for model building, analysis, and parameter estimation in systems biology and neuroscience. *Neuroinformatics*, 1–19. doi:10.1007/s12021-021-09546-3.
- Sobol, I.M. (2001). Global sensitivity indices for nonlinear mathematical models and their Monte Carlo estimates. *Math. Comput. Simul.*, 55(1-3), 271–280. doi:10.1016/S0378-4754(00)00270-6.
- Tennøe, S., Halmes, G., and Einevoll, G.T. (2018). Uncertainty: A python toolbox for uncertainty quantification and sensitivity analysis in computational neuroscience. *Front. Neuroinform.*, 12, 49. doi:10.3389/fninf.2018.00049.
- Tikhonov, A.N. (1943). On the stability of inverse problems. *Dokl. Akad. Nauk SSSR*, 39(5), 195–198.
- Zi, Z. (2011). Sensitivity analysis approaches applied to systems biology models. *IET Syst. Biol.*, 5(6), 336–346. doi:10.1049/iet-syb.2011.0015.